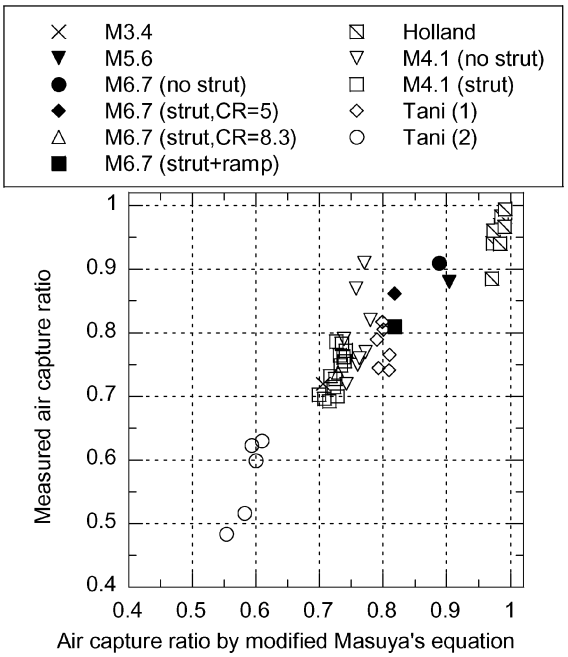

Fig. 3 Mass-capture ratio predicted by modified Masuya equation.

waves increases. The number increases with increasing contraction ratio.

In the data, h_e was from 80 to 100% of h; L was from 0% to 50% of the length from the inlet entrance to the throat; l was from 9% to 27% of the inlet length; SW was from 30 to 60 deg; and CR was from 2.9 to 9.3. Width at the entrance was not selected as a parameter because the widths of the inlets adopted here were in a narrow range, from 0.8 to 1 of the inlet height.

The modified mass-capture ratio $\eta_{\text{cap},m}$ was expressed using the modification factor f and the parameters $n1 = 10$, $n2 = 0.4$, $n3 = 1$, $n4 = 0.1$, and $n5 = 0.5$:

$$\eta_{\text{cap},m} = (\eta_{\text{cap}}\,[\text{by Masuya's equation}]) \times f(x) \tag{4}$$

$$x = \left(\frac{h_e}{h}\right)^{10}\left(\frac{h_e}{L}\right)^{0.4}\left(\frac{L-\ell}{L}\right)\left(\frac{90-SW}{90}\right)^{0.1}\left(\frac{1}{CR}\right)^{0.5} \tag{5}$$

The modification factor was attained empirically from the data of the mass-capture ratios:

$$f = -0.0092/x + 1.05 \tag{6}$$

Figure 3 shows the correlation between the test data and the calculated capture ratio by Masuya's equation. Correlation between the experimental values and the calculated values was 0.94.

Equation (5) shows that the effect of the boundary layer on the capture ratio was large. The inflow boundary layer should be thin. The effect of the strut was also large. Neither the effect of the swept angle nor the length of the inlet affected the mass-capture ratio greatly.

Conclusions

Air-mass capture ratios of the scramjet inlet models were measured in the PWT at Mach 3.4, 5.3, and 6.7 conditions. The ratios of the RJTF test models were estimated with the test data from the PWT. An empirical equation was constructed for the mass-capture ratio of the sidewall-compression-type inlets. The equation showed that the effect of the boundary layer and the effect of the strut were large.

References

[1]Chinzei, N., "Research Activities on Scramjets at NAL-KRC in Japan," 15th International Symposium on Air Breathing Engines, ISABE 2001-1075, Sept. 2001.

[2]Hudgens, J. A., and Trexler, C. A., "Operating Characteristics at Mach 4 of an Inlet Having Forward-Swept, Sidewall-Compression Surfaces," AIAA Paper 92-3101, July 1992.

[3]"Measurement of Gas Flow by Means of Critical Flow Venturi Nozzles," ISO9300, 1990.

[4]Masuya, G., and Wakamatsu, Y., "Calculation of Scramjet Performance," National Aerospace Lab., NAL TR-987, Tokyo, Japan, July 1988 (in Japanese).

[5]Holland, S. D., "Computational Parametric Study of Sidewall-Compression Scramjet Inlet Performance at Mach 10," NASA TM 4411, Feb. 1993.

[6]Kanda, T., Komuro, T., Masuya, G., Kudo, K., Murakami, A., Tani, K., Wakamatsu, Y., and Chinzei, N., "Mach 4 Testing of Scramjet Inlet Models," *Journal of Propulsion and Power*, Vol. 7, No. 2, 1991, pp. 275–280.

[7]Tani, K., Kanda, T., Kudou, K., Murakami, A., Komuro, T., and Ito, K., "Aerodynamic Performance of Scramjet Inlet Models with a Single Strut," AIAA Paper 93-0741, Jan. 1993.

[8]Tani, K., Kanda, T., and Tokunaga, T., "Starting Characteristics of Scramjet Inlets," *Proceedings of 11th International Symposium on Air-Breathing Engines*, Vol. 1, AIAA, Washington, DC, 1993, pp. 1071–1080.

Nucleation Mechanism for Freezing of Alumina in Solid Propellant Rocket Motor Nozzles

Daniel E. Rosner*
Yale University, New Haven, Connecticut 06520-8286

I. Introduction, Background, Objectives

IT is well known that the addition of appreciable amounts of aluminum powder (e.g., ca. 15–20 wt.%) to conventional double-base solid propellants can improve their performance (e.g., specific impulse, etc.).[1] However, the achievable performance gain will certainly depend upon the location of the release of the heat of molten alumina crystallization during the droplet-laden gas expansion process.[2] Moreover, the location of alumina freezing will also dramatically influence the optical properties of such plumes.[3,4] Until now, there has evidently been no simple method to estimate the spatial location and distribution of the volumetric rate of release of this appreciable latent heat. While undercoolings of as much as around 20% of the equilibrium freezing point[5,6] are known to be possible in principle, actual performance experience indicates that such extreme delayed freezing probably does not occur, at least for the bulk of the alumina present. In this Note we propose a plausible explanation for this, and one which, with further development, promises to enable rational predictions of crystallization rates in metallized solid-(propellant)-rocket-motor (SRM) combustion products.

II. Theory of Alumina Nanodroplet Freezing

Using typical numbers for aluminized SRM situations [e.g., the space shuttle solid rocket boosters (SRBs); compare Table 1], we

Received 23 September 2003; accepted for publication 28 October 2003.

*Professor, Center for Combustion Studies, Chemical and Mechanical Engineering, and Engineering Consultant, Mason Laboratory, 9 Hillhouse Avenue; daniel.rosner@yale.edu.

show here that premature freezing of nanodroplets of alumina [the so-called condensation mode, with a Sauter mean diameter (SMD) d_{32} of only about 56 nm (Ref. 7)] can limit supercooling of the bulk of the [supermicron mode(s) of] molten alumina present in the nozzle. The nanodroplet population, resulting from the condensation of molecular vapor precursors to Al_2O_3, is expected to freeze first because, even though they might supercool by, say, 19% of *their* equilibrium mp, *their* equilibrium mp is itself appreciably elevated by the Laplace overpressure associated with their surface energy and small radii.[8] The freezing point shift is, in turn, caused by the appreciable volume contraction upon freezing—estimated to be about 30% for alumina. This remarkable combination of circumstances is shown next to enable the freezing of an adequate fraction of the nanodroplet population to heterogeneously nucleate freezing of the micron-sized alumina droplets at temperatures well above $0.81(2327\ \text{K}) = 1885$ K (which might otherwise have been necessary).

With this picture in mind, we first estimate the equilibrium freezing point of a nanodroplet of diameter d at external pressure p by combining the equation for the Laplace (capillary) overpressure: $(\Delta p)_L = 2\gamma_{LV}/(d/2)$ (where γ_{LV} is the liquid/vapor interfacial energy) with an integrated form of the Clausius–Clapeyron equation, based on the assumption that the property combination $\mathcal{L}$ [defined by Eq. (1)] is nearly constant.

$$\mathcal{L} \equiv [(\Delta H_m/V_s)/(\Delta V_m/V_s)] \cdot p_{\text{ref}} \approx 1.36 \times 10^4 \tag{1}$$

This leads to the following equation for $T_{\text{mp}}(d, p)$, where $T_{\text{mp,ref}} \equiv T_{\text{mp}}(\infty, 1\ \text{atm}) = 2327$ K, with typical results plotted in Fig. 1:

$$T_{\text{mp}}(d, p) = T_{\text{mp}}(\infty, 1\ \text{atm}) \cdot \exp\{(1/\mathcal{L}) \cdot \{[(\Delta p)_L/p_{\text{ref}}] + (p/p_{\text{ref}}) - 1\}\} \tag{2}$$

At any location within the nozzle, an inverted form of this equation was used to find the size of the nanodroplet that satisfies the local homogeneous nucleation (crystallization) condition: $T = 0.81T_{\text{mp}}(d; p)$, where T is the local gas mixture temperature achieved in the isentropic expansion from the assumed chamber conditions (Table 1).

Table 1 SRM environment and alumina property values for illustrative calculations (Figs. 1, and 2)

Quantity	Value used
SRM (e.g., SS-SRB) environment[1]	
Chamber pressure	68 atm (6.9 MPa)
Chamber temperature	3400 K
Mean molecular weight	29
Mean specific heat ratio	1.15
Aluminum mass loading (fuel)	0.16
Alumina mass fraction (products)	0.33
SMD-nanodroplet mode	56 nm
SMD-microparticle mode	3.6 microns
Estimated alumina property values	
Molecular weight	101.96
$T_{\text{mp,ref}}$ (1 atm, $d = \infty$)	2327 K
Heat of fusion at $T_{\text{mp,ref}}$	107.5 MJ/kg-mole
Molar volume of solid at mp, ref	2.6×10^{-2} m^3/kg-mole
Relative volume change on melting	0.3 ($\Delta V_m/V_s$)
Surface energy of melt/vapor	0.9 J/m^2

III. Physical/Mathematical Model

With the preceding objectives in mind, we now investigate a deliberately idealized mathematical model[9] of the nonequilibrium crystallization of an initially log-normal population of alumina nanodroplets present at negligible mass loading in an expanding mixture of combustion products (including micron-sized alumina droplets). On the timescale of product gas expansion (around milliseconds), crystallization of each nanodroplet is considered instantaneous. (Once nucleation occurs, crystallization should take less than around 0.2 μs for a 56-nm-diam droplet cooled to $0.81T_{\text{mp}}$.) However, as just noted, each such droplet is considered to crystallize at a size-dependent temperature: $0.81T_{\text{mp}}(d; p)$, where $T_{\text{mp}}(d; p)$, now given by Eq. (2). Exploiting an isentropic approximation, we account for the thermal coupling between these nanodroplets and the expanding carrier fluid, approximated as an ideal gas-particle mixture with nearly constant specific heat ratio. Nanodroplet number densities are considered low enough to neglect appreciable Brownian coagulation/heterogeneous nucleation during the expansion.

For our present quantitative estimates we considered an initial nanodroplet population with a SMD of around 56 nm and a volume distribution function spread parameter of around $\sigma_g = 2.1$. This coagulation-aged spread (for example, see Refs. 10 and 11) immediately leads to an estimate of the geometric mean size d_g (around 48 nm) for the nanodroplet population, from which we can then find the number fraction that is frozen g at any expansion ratio (pressure ratio p_{ch}/p):

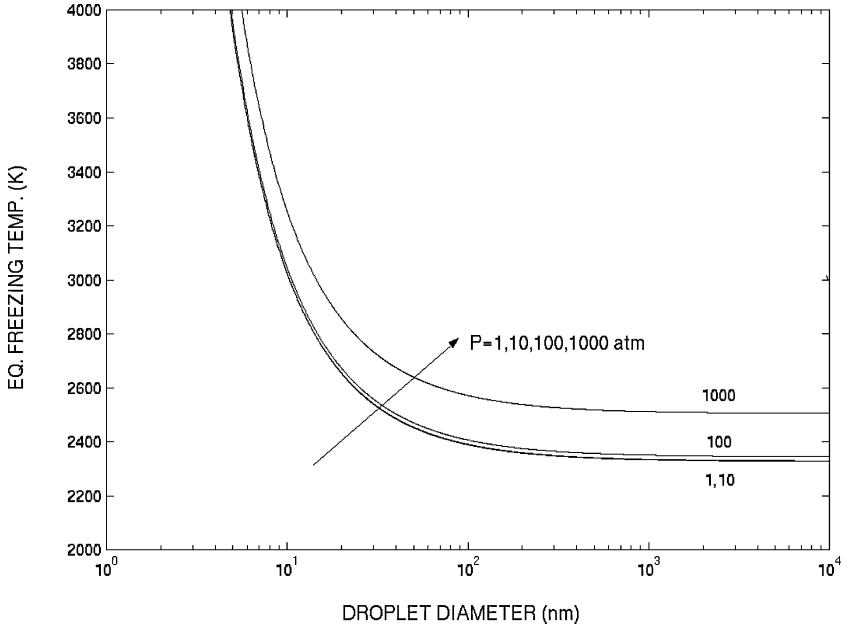

Fig. 1 Estimated equilibrium freezing temperatures of alumina nanodroplets of diameter d (nm) at several external pressure levels (atm).

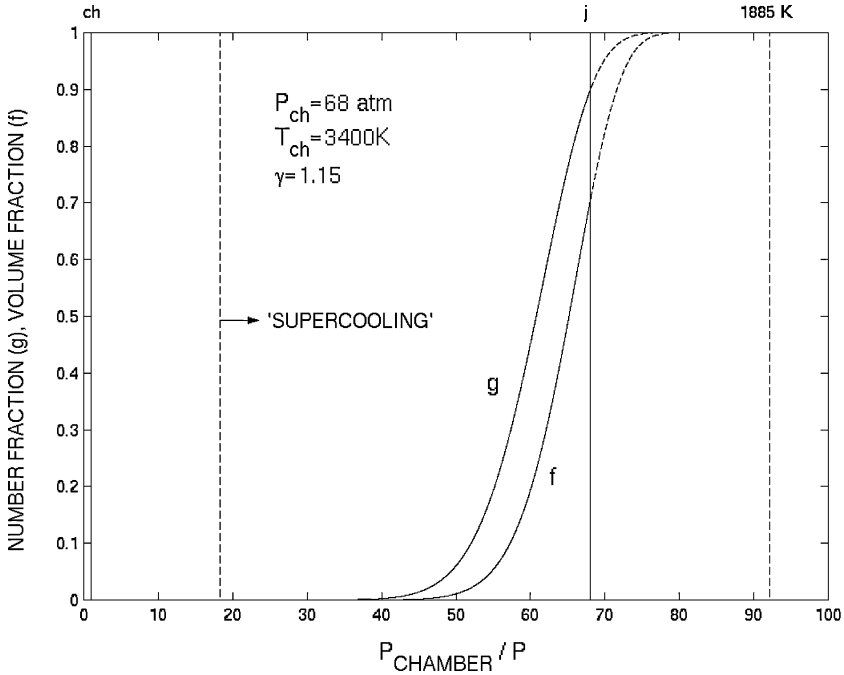

Fig. 2 Predicted evolution of nanodroplet freezing during the expansion of aluminized SRM combustion products: $g \equiv$ number fraction frozen [Eq. (3)] and $f \equiv$ volume fraction frozen. Also shown are the expansion pressure ratios p_{ch}/p at which $T = T_{mp,ref} = 2327$ K (within nozzle) and $T = (0.81) \cdot T_{mp,ref} = 1885$ K (downstream of nozzle exit plane; station j).

$$g = (1/2) \cdot \left\{1 + \mathrm{erf}\left[\ell_n(d/d_g)^3 \Big/ \left(\sqrt{2} \cdot \ell_n \sigma_g\right)\right]\right\} \qquad (3)$$

d/d_g and the nanodroplet population spread also allows us to calculate the corresponding volume fraction[11] f, which is frozen—for completeness, this quantity is also shown in Fig. 2. We also comment that, although it is true that the very smallest droplets in the postulated *nd* population are unstable with respect to vaporization (because of the Gibbs–Kelvin effect on equilibrium vapor pressure), they are found to comprise an insignificant fraction of the total *nd* population (even at 3400 K).

Notice that by an expansion ratio of only about 52 (where the local gas temperature is about 2030 K, corresponding to the bulk of the alumina being undercooled by at most only about 13%) over 10% of the nanoparticle population should be frozen. Moreover, their sublimation lifetime would be more than adequate to survive, even in the absence of any local condensible vapor. What remains is the need to estimate whether the corresponding local number concentration of freezing nucleii would be able to bring about freezing of the local supermicron population on a microsecond timescale.

IV. Application to the Heterogeneous Nucleation of Crystallization in the SS-SRB Environment

Of course, we need to learn more about the efficacy of nanoparticles as freezing nucleii for the much larger but much less numerous alumina microdroplets present in aluminized-SRM applications. But, let us now suppose that the decisive rate of release of the heat of crystallization will be controlled by the availability of these postulated nanoparticle freezing nucleii, that is, their collision rates with supermicron, undercooled suspended alumina droplets.

Previous work[2] has shown that the supermicron mode cannot quite accelerate as fast as the carrier gas, so that by the time these droplets start to supercool the local gas mixture is already moving faster than the droplets by slip velocities U_{slip} of the order of 10^2 m/s. Then a lower limit to the characteristic time between *np*/microdroplet (μd) encounters is set by the local value of

$$t_{np/\mu d} = \left[g \cdot N_{nd} \cdot U_{slip} \cdot \eta_{cap} \cdot (\pi/4) d_{\mu d}^2\right]^{-1} \qquad (4)$$

where η_{cap} (the capture fraction[9,12]) is taken to be unity. To complete this calculation, we require an estimate of the effective total number density of nanodroplets present prior to the expansion, that is, $N_{nd,ch;eff}$, and then this should be reduced by the gas density ratio $(p_{ch}/p)^{-1/\gamma}$, where $\gamma = 1.15$ (Table 1). (For simplicity, we do not consider here the likelihood of continuous formation of *nd*s during the expansion.)

We proceed by first recalling that the total alumina mass fraction in the combustion products is about 0.33. It has also been reported[7] that the surface area associated with the condensation mode is about one-third of that of the micron-sized particles. This information, combined with the preceding SMDs, fortunately allows us to fix an order of magnitude for $N_{nd,ch}$, which we find to be $0.6 \times 10^{17} \mathrm{m}^{-3}$ or about $N_{nd} = 3 \times 10^{16}$ m^{-3}, where $g = 0.1$. Using these estimates in Eq. (4) for $t_{np/\mu d}$ reveals that crystallization induced by *np* contacts could indeed take place on about a 3-μs timescale, corresponding to release of the heat of crystallization in less than 1 cm of further axial travel, that is, within the nozzle.

The present preliminary estimates evidently justify more accurate predictions in the immediate future. Apart from some basic data that are undoubtedly still controversial (such as the actual np/nd concentration near the exit plane), these predictions, in turn, ultimately require integrations over both the distributions of frozen nanoparticles (here assumed to be a truncated log-normal) and the slipping molten microdroplets, and allow for both incomplete capture (i.e., $\eta_{cap} < 1$) and a distribution of nucleant potency in the nanoparticle population. Additional details will be presented in a full-length account of this new approach,[9] which is only outlined here.

V. Results, Discussion, Implications

It is remarkable, and somewhat ironic, that lag phenomena associated with the inertia of the supermicron droplets (comprising most of the mass of suspended alumina) responsible for calculable performance losses appear to be essential to increase the collision frequency between nano- and microparticles to levels required for microdroplet freezing on a microsecond timescale. Indeed, in the limit $U_{slip} \to 0$ our estimates of the characteristic time $t_{np/\mu d}$ [compare Eq. (4)] would be in the millisecond range because collision rates would then be limited by the much slower process of nanoparticle diffusion (because of their Brownian motion).[9,12]

The relations and simplifications just utilized were intended only to be sufficient to establish the plausibility of the present mechanism for crystallization heat release in metallized SRM situations. If this concept can now be more firmly demonstrated, many systematic

improvements can/should be introduced with the goal of increasing the accuracy and generality of our present predictions. This includes allowance for the variability of materials properties (like $\Delta H_m / V_s$, surface energy, specific heat ratio, etc.), which we have, for simplicity, treated as constant (compare Table 1). It would also be possible and necessary to calculate volumetric crystallization heat-release rates by integrating over both the distributions of frozen nanoparticles and molten microdroplets, and, of course, include the effects of this heat release on the expanding carrier gas. Accurately estimating microdroplet temperatures and velocities in the expanding flow now takes on even greater significance because of its key role in determining the collision frequency between our predicted nanoparticles and the more familiar micrometer mode that dominates the local particle mass fraction. Ultimately, it might also be possible to take into account the likelihood that all nanoparticles will not be equally effective as freezing nucleii when they encounter supercooled microdroplets. We anticipate that questions of this type, as well as the liklihood of the nucleation of new nanodroplets/particles during the expansion, will motivate interesting new research, with results also applicable to other fields in which this sequence of crystallization events is also likely.

VI. Conclusions

In summary, our preliminary estimates have indicated that during the solid-rocket-motor (SRM) combustion product expansion process numerous/mobile nanocrystals are formed by the homogeneous nucleation of crystallization. Because of the Laplace overpressures existing within the alumina nanodroplets, these are expected to freeze surprisingly early [Eqs. (1) and (2) and Fig. 1], and some nanoparticle freezing nuclei might already be present near the equilibrium freezing point of the bulk of the molten alumina. With further expansion the number of these frozen nanoparticles, metastable with respect to local sublimation,[9] is predicted to increase rapidly until their collisions with supercooled microdroplets brings about heterogeneously nucleated crystallization well above microdroplet temperatures near 1885 K and on a microsecond timescale. Our preliminary estimates (Sec. V and Fig. 2) indicate that this "avalanche of freezing" will ordinarily occur before the nozzle exit plane (station j, Fig. 2) is reached.

We have called attention here to the likely importance of nanodroplet freezing in providing abundant nuclei, metastable with respect to sublimation, for the crystallization of the bulk of the alumina produced in the combustion expansion of aluminized solid propellants. Our preliminary calculations, just summarized, suggest that the decisive rate of release of the heat of crystallization will generally be controlled by the availability of these nanoparticle freezing nucleii, that is, their collision rates with supermicron, undercooled suspended alumina droplets. With further development, this tractable scenario, which appears to be plausible and self-consistent and now cries out for more direct experimental supporting evidence, promises to enable rational predictions of crystallization locations/rates in metallized-SRM combustion products.

In closing, we remark that, although the engineered metallized-SRM environment has many novel features, the sequence of events considered quantitatively in this Note (i.e., freezing by homogeneous nucleation of the nanodroplet mode first, thereby providing a population of freezing nuclei for the bulk of the suspended molten material) will probably apply to other important environments, including natural ones, in which rapid cooling of a complex, multimodal suspension of liquid in vapor occurs by a combination of expansion, entrainment, and/or IR radiation.

Acknowledgments

It is a pleasure to acknowledge helpful discussions with P. C. Nordine (Containerless Research, Inc.), R. A. Reed (Arnold Engineering Development Center), D. T. Wu and J. Wettlaufer (Yale University), R. L. McGraw (Brookhaven NL), H. S. Pergament (PST Inc.), and the assistance of M. Zurita-Gotor in making the illustrative calculations presented in Figs. 1 and 2.

References

[1]Sutton, G. P., *Rocket Propulsion Elements*, 6th ed., Wiley, New York, 1992.

[2]Henderson, C. B., "Effect of Crystallization Kinetics on Rocket Performance," *AIAA Journal*, Vol. 15, No. 4, 1977, pp. 600–602.

[3]Carlson, D. J., "Emittance of Condensed Oxides in Solid Propellant Combustion Products," *Proceedings of the Tenth International Combustion Symposium*, Combustion Inst., Pittsburgh, PA, 1965, p. 1424.

[4]Dill, K. M., Reed, R. A., Calai, V. S., and Schulz, R. J., "Analysis of Crystalline Phase Aluminum Oxide Particles from Solid Propellant Exhausts," *Journal of Propulsion and Power*, Vol. 6, No. 5, 1990, pp. 668–671.

[5]Weber, J. K. R., Anderson, C. D., Merkley, D. R., and Nordine, P. C., "Solidification Behavior of Undercooled Liquid Aluminum Oxide," *Journal of the American Ceramic Society*, Vol. 78, No. 3, 1995, pp. 577–582.

[6]Rosner, D. E., and Epstein, M., "Simultaneous Kinetic and Heat Transfer Limitations in the Crystallization of Highly Undercooled Melts," *Chemical Engineering Science*, Vol. 30, 1975, pp. 511–520; also *International Journal of Heat and Mass Transfer*, Vol. 36, No. 12, 1993, pp. 2987–2995.

[7]Beitung, E. J., "Solid Rocket Motor Exhaust Model for Alumina Particles in the Stratosphere," *Journal of Spacecraft and Rockets*, Vol. 34, 1997, pp. 303–310, pp. 311–317.

[8]deFay, R., Prigogine, I., Bellemans, A., and Everett, D. H., *Surface Tension and Adsorption*, Wiley, New York, 1966.

[9]Rosner, D. E , "Theory for the Nonequilibrium Crystallization of a Population of Nano-Droplets Which Become Freezing Nucleii in Rapidly Expanding Gas/Micro-Droplet Flows," *Journal of Propulsion and Power* (to be published).

[10]Rosner, D. E., and Khalil, Y. F., "Particle Morphology and Knudsen Transition Effects on Thermophoretically-Dominated Total Mass Deposition Rates from Coagulation-Aged Populations," *Journal of Aerosol Science*, Vol. 31, No. 3, 2000, pp. 273–292.

[11]Rosner, D. E., and Tassopoulos, M., "Deposition Rates from Polydispersed Particle Populations of Arbitrary Spread," *AIChE Journal*, Vol. 35, No. 9, 1989, pp. 1497–1508.

[12]Rosner, D. E., *Transport Processes in Chemically Reacting Flow Systems*, Dover, New York, 2000, Secs. 6.6.1 and 8.2.2.

Among other minerals of geophysical interest, Shen, G., and Lazor, P. [J. Geophys. Res., Vol. 100, No. B9, pp. 17,699–17,713 (Sept. 10, 1995)] have experimentally studied the melting point of macroscopic specimens of corundum (AI203) up to nearly 30 GPa (ca. 300,000 atm), using a laser-heated diamond anvil cell. While melting temperatures above 3600 K were, indeed, reported (cf. Fig. 1), in their anvil apparatus this required pressures above ca. 24 GPa. This seems to be the only available high pressure melting point data for alumina, but it indicates that subsequent rocket motor calculations based on the mechanism of nano-particle freezing suggested here will have to introduce more realistic high pressure property data, only now becoming available.